Available online at www.sciencedirect.com
SCIENCE @ DIRECT®

Journal of Fluorine Chemistry 124 (2003) 99–104

JOURNAL OF FLUORINE CHEMISTRY
www.elsevier.com/locate/jfluchem

Ab initio investigations of the C_2F_4S isomers and of their interconversions

Irene Shim*, Sandra Vallano-Lorenzo[1], Pilar Lisbona-Martin[1], Alexander Senning[2]

Department of Chemistry, Technical University of Denmark, DTU 207, DK-2800 Kgs. Lyngby, Denmark

Received 22 April 2003; received in revised form 10 July 2003; accepted 13 July 2003

Abstract

The transition states and the activation energies for the unobserved isomerization reactions between the three possible C_2F_4S isomers with divalent sulfur, trifluorothioacetyl fluoride **1**, tetrafluorothiirane **2**, and trifluoroethenesulfenyl fluoride **3**, have been determined by ab initio Hartree-Fock (HF), Møller-Plesset second-order perturbation (MP2) calculations and by Gaussian-3 theory. The results show that the unobserved isomerization reactions are feasible. Furthermore, all three isomers should exist as stable species, but the unknown isomer, **3**, is considerably less stable than the known isomers, **1** and **2**.

Keywords: Ab initio Hartree-Fock; Møller-Plesset second-order; Gaussian-3 theory; Transition state; Activation energy; Trifluorothioacetyl fluoride; Tetrafluorothiirane; Trifluoroethenesulfenyl fluoride

1. Introduction

The three possible C_2F_4S isomers with divalent sulfur, trifluorothioacetyl fluoride **1**, tetrafluorothiirane **2**, and trifluoroethenesulfenyl fluoride **3**, have been investigated by ab initio Hartree-Fock (HF), Møller-Plesset second-order perturbation (MP2) calculations, and by Gaussian-3 theory [1], G3(MP2), calculations using the programs SPARTAN PRO [2] and Gaussian 98 (see Gaussian 98, revision A.11.2 [3]).

2. Results and discussion

The chlorine analogs of the molecules presented in Fig. 1 are all known [4]. Of the fluorine compounds, only **1** [5] and **2** [6–10] are known. Compound **2** has been prepared from thiocarbonyl difluoride and hexafluoropropylene oxide [6,7]. With catalysts that catalyze free radical pathways **2** forms well-defined polymers [7,8]. Polymers of **2** have been described as a coating material for razor blades [9].

The structure of **2** has been deduced from gas phase electron diffraction measurements [10] carried out on a mixture of **2** and octafluorocyclobutane. In Table 1 the results obtained from the electron diffraction measurements by least square fittings are compared with the optimized structures as determined in our HF calculations using four different basis sets ranging from 6–31G* to 6–311 + G*. Also included are the corresponding results obtained from MP2 calculations with and without frozen core. The results presented in Table 1 show reasonable agreement with the experimental data. All the calculated distances deviate by less than 0.02 Å from the experimental values. The discrepancies between the calculated and the experimental values for the angles are less than 1° for ∠CSC, ∠SCC, and ∠FCF but for ∠SCF and ∠CCF the discrepancies are close to 3°. As the calculated values for the angles deviate by less than 1° from one another it appears possible that the experimental values for ∠SCF and ∠CCF are inaccurate. It is especially noted that there are no significant discrepancies between the results obtained in HF and MP2 (full) calculations with the basis set 6–31G*. These methods are employed in G3(MP2) when optimizing the geometry and determining the vibrational frequencies used when deriving the thermal data.

HF, MP2, and G3(MP2) calculations have been carried out for all the molecules and transition state structures investigated. All the transition states are identified by the presence of one negative eigenvalue of the Hessian matrix. These negative eigenvalues define reaction paths, and by following these paths it has been verified that the reaction paths identified in the present work do connect the reactants with the products. Mulliken population analyses have been

---

* Corresponding author. Tel.: +45-4525-5432; fax: +45-4588-3136.
E-mail addresses: irene.shim@kemi.dtu.dk (I. Shim), alexander.senning@kemi.dtu.dk (A. Senning).

[1] On leave from the Department of Chemical and Environmental Engineering, Centro Politécnico Superior, University of Zaragoza, C/María de Luna 3, E-50015 Zaragoza, Spain.

[2] Co-corresponding author.

0022-1139/$ – see front matter © 2003 Elsevier B.V. All rights reserved.
doi:10.1016/S0022-1139(03)00196-9

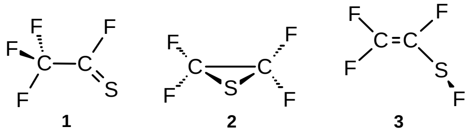

Fig. 1. The C_2F_4S isomers with divalent sulfur.

performed for both the stable molecules and the transition state structures.

The total energies derived when optimizing the geometries in HF calculations, as well as the energies obtained in MP2 calculations, of the equilibrium structures determined in the HF calculations are provided in Appendix A. Also included are the total energies derived by performing full MP2 and G3(MP2) calculations.

The rotational barriers around the C–C single bond in **1**, and the C–S single bond in **3** have been investigated by minimizing the energy in HF calculations as the dihedral angles are changed systematically, and thereafter performing MP2 calculations on the resulting geometries. The rotational barrier around the C–C single bond in **1** is derived as 5.3 kJ mol^{-1}, which indicates free rotation around this bond. Fig. 2 shows the rotational barrier around the C–S single bond in **3**. For this molecule the rotational barrier is 42.6 kJ mol^{-1}. The most stable conformer of **3**, **3**(1), is nonplanar, and the dihedral angle C(1)–C(2)–S–F(1) is 97.3°. The conformers **3**(2) and **3**(3) are both planar, as shown in Fig. 3. The large rotational barrier is connected with the change of the symmetry from C_1 to C_s. This is reflected in the highest occupied molecular orbital, HOMO. It is observed that this orbital in the planar molecule, C_s symmetry, can be characterized as an antibonding orbital between the C–C bonding π orbital and a lone pair on S, while the orbital HOMO-1 is the corresponding bonding combination. As the dihedral angle is increased from 0° or decreased from 180°, a bonding interaction occurs between the C–C bonding π orbital and a lone pair on S in both HOMO and HOMO-1.

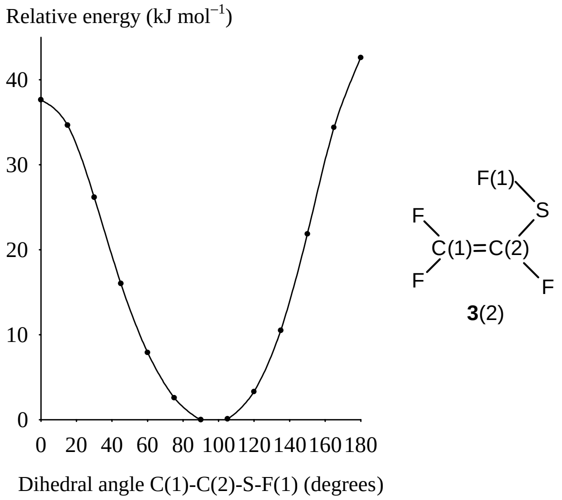

Fig. 2. The rotational barrier around the C–S single bond in **3** as derived in MP2 calculations. Also shown is **3** with the dihedral angle C(1)–C(2)–S–F(1) equal to 0°.

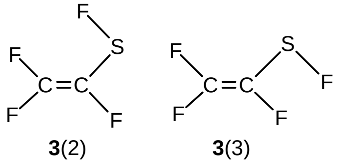

Fig. 3. The two planar conformers of compound **3**, **3**(2) and **3**(3).

The energy barrier around the C–S single bond in ethenethiol has been investigated in HF and MP2 calculations analogous to those performed for **3**. For ethenethiol the energy barrier amounts to 9.7 kJ mol^{-1}, and the top of the barrier occurs when the dihedral angle C–C–S–H is 71.2°. The most stable conformer of ethenethiol is the analog of **3**(2) while the analog of **3**(3) has an energy that is 3.1 kJ mol^{-1} higher. It is observed that the HOMO of ethenethiol is antibonding between the C–C bonding π orbital and a lone pair on S, and contrary to **3** this orbital does not increase its bonding contribution as the dihedral angle is changed. The HOMO-1 is a C–C–S bonding π

Table 1
Structural data for tetrafluorothiirane **2**

Distances and angles	Experimental [4]	Theoretical					
		HF				MP2/6–31G*	
		6–31G*[a]	6–31 + G*[a]	6–311G*[b]	6–311 + G*[b]	Frozen core[a]	Full[b]
C–S (Å)	1.799(3)	1.790	1.787	1.789	1.790	1.809	1.806
C–C (Å)	1.45(1)	1.462	1.467	1.463	1.467	1.465	1.463
C–F (Å)	1.322(2)	1.314	1.315	1.309	1.309	1.344	1.342
∠CSC (°)	47.5(5)	48.2	48.5	48.3	48.4	47.8	47.8
∠SCC (°)	66.2(3)	65.9	65.8	65.9	65.8	66.1	66.1
∠FCF (°)	109.1(7)	109.8	109.5	109.7	109.6	109.7	109.8
∠SCF (°)	121.5(6)	118.9	119.1	118.8	118.9	118.6	118.6
∠CCF (°)	116.2(5)	118.8	118.9	118.9	119.0	119.0	119.0

[a] Calculations have been performed using SPARTAN PRO [2].

[b] Calculations have been performed using Gaussian 98 [3].

Table 2
The relative energies, ΔE, enthalpies, ΔH, and Gibbs free energies, ΔG, in kJ mol^{-1} of the C_2F_4S isomers **1**–**3**, as derived in MP2 and G3(MP2) calculations

Compound	Name	Symmetry	MP2, 6–31G*		G3(MP2)			
			HF geometry (frozen core) (ΔE)	Full optimized (ΔE_e)	ΔE_e	ΔE_0	$\Delta H_{298.15}$	$\Delta G_{298.15}$
1	Trifluorothioacetyl fluoride	C_s	0	0	0	0	0	0
2	Tetrafluorothiirane	C_{2v}	86	88	76	76	75	81
3(1)	Trifluoroethenesulfenyl fluoride	C_1	198	197	160	156	157	155
3(2)	Trifluoroethenesulfenyl fluoride	C_s[a]	236	236	201	197	197	
3(3)	Trifluoroethenesulfenyl fluoride	C_s[a]	241	241	205	200	200	
	Thioacetaldehyde	C_s	0	0	0	0	0	0
	Thiirane	C_{2v}	5	5	8	12	10	14
	Ethenethiol	C_s[a]	42	41	13	7	8	7
	Ethenethiol	C_1	44	43	14	8	9	8

Also included are the relative energies of the corresponding hydrogenated molecules.

[a] The molecule is planar.

orbital in the planar conformations, and it appears to be the least bonding when the dihedral angle C–C–S–H is 71.2°.

Table 2 shows the relative energies of **1**, **2**, and **3**, as derived from MP2, and G3(MP2) calculations. Data for two additional characteristic conformers of **3** are also included. Furthermore, Table 2 shows the values for ΔE_0 as well as the relative enthalpies and Gibbs free energies derived in G3(MP2) calculations. In addition, Table 2 shows the relative stabilities of the corresponding hydrogen analogs of **1**, **2**, and **3**, i.e. thioacetaldehyde, thiirane, and ethenethiol.

The ΔE values reported in Table 2 are derived from MP2 frozen core calculations based on the geometries optimized in HF calculations, and the ΔE_e values are derived by optimizing the molecular geometry in full MP2 calculations. It is noted that the discrepancies between the ΔE and ΔE_e values, as derived in the MP2 calculations, amount to at most 2 kJ mol^{-1}. G3(MP2) calculations include various corrections and the decreases in the ΔE_e values as derived in G3(MP2) relative to the MP2 calculations are due mainly to the basis set corrections included in the G3(MP2) method. In G3(MP2) theory, the zero point energy is derived using the normal frequencies determined in HF calculations with the basis set 6–31G* but scaled by 0.8929. Furthermore, the ideal gas law is used when deriving the enthalpies and the Gibbs free energies. Table 2 shows that **1** is the most stable isomer followed by **2**, and that **3** is the least stable of the isomers. It is observed that the energy separations between the fluorinated isomers are much larger than those between the corresponding hydrogen compounds. The decrease in the ΔE_e values between thioacetaldehyde and ethenethiol as derived in G3(MP2) relative to the MP2 calculations is 28 kJ mol^{-1} as compared with the corresponding value of 37 kJ mol^{-1} between **1** and **3**(1). In both cases the decrease is due mainly to the corrections for the basis set amounting to 23.3 kJ mol^{-1} and 29.8 kJ mol^{-1} for the perhydrogenated and the perfluorinated species, respectively. Correspondingly, the correction due to correlation amounts to 4.8 kJ mol^{-1} for the perhydrogenated species and to 6.6 kJ mol^{-1} for the perfluorinated species.

The isomerization reactions studied are those in which a given compound is transformed into a more stable species. Therefore, three reactions are possible: **3** → **1** (1); **3** → **2** (2); and **2** → **1** (3).

The transition state of each reaction has been identified, and Table 3 shows the activation energies, enthalpies, and Gibbs free energies derived. Also included are energies, enthalpy and Gibbs free energies that are required for homolytic bond cleavage of the S–F bond in **3**. The discussion of the geometries of the transition states below is based on the results of the full MP2 calculations and the Mulliken charges reported are obtained in HF calculations using basis sets that include both polarization and diffuse functions.

Scheme 1 shows the transition state identified in the isomerization reaction (1), TS(1).

Table 3
Activation energies, ΔE, enthalpies, ΔH, and Gibbs free energies, ΔG (kJ mol^{-1}) as derived in MP2 and G3(MP2) calculations

Isomerization reaction	Transition state	MP2	MP2	G3(MP2)			
		HF geometry (frozen core) (ΔE)	Optimized (full) (ΔE_e)	ΔE_e	ΔE_0	$\Delta H_{298.15}$	$\Delta G_{298.15}$
3 → **1** (1)	TS(1)	177	180	188	184	182	187
3 → **2** (2)	TS(2)	303	287	277	272	271	275
2 → **1** (3)	TS(3)	225	224	214	209	209	207
$3 \rightarrow {}^2F + {}^2CF_2 = CFS$		304	315	308	298	301	263

Also included are the corresponding values for the homolytic bond cleavage of the S–F bond in **3**.

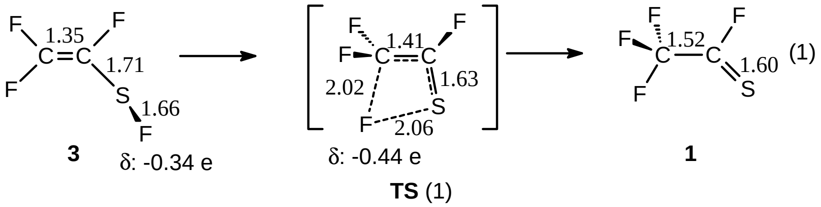

Scheme 1. The isomerization reaction **3** → **1**.

The difference in Gibbs free energy, $\Delta G_{298.15}$, in reaction (1) is 187 kJ mol^{-1}. This is the smallest of the ΔG values derived for the three isomerization reactions studied but it is so large that both molecules, **1** and **3**, should exist as stable species. The displacement vectors of the imaginary frequency determined in TS(1) clearly show that the F atom approaches the C atom to which it finally becomes bound in **1**. In TS(1) the S atom is out of the plane defined by the two C atoms and the three F atoms in **3**. The distance between the F atom that is attached to S in **3** and to C in **1** has increased from 1.66 to 2.06 Å, and the distance to the C atom to which F becomes attached in **1** has decreased from 3.47 Å in **3** to 2.02 Å. Although this is still considerably longer than the final C–F distance in **1** of 1.34 Å, the F atom that is bonded to S in **3** has approached the C atom to which it becomes bound in **1**. The C–C distance in TS(1) is 1.41 Å which is in between the length of the C=C double bond in **3**, 1.35 Å, and that of the C–C single bond in **1**, 1.52 Å. The C–S distance is 1.63 Å, and this is closer to that of the product **1**, 1.60 Å, than to that of the reactant **3**, 1.71 Å. According to a Mulliken population analysis, the F atom that is attached to S in **3** has acquired a charge of $-0.44e$ in TS(1). In the transition state the F atom that is attached to S in **3** and to C in **1** is only weakly bonded.

A possible transition state, TS(2), has been identified for the isomerization of **3** to **2** as shown in reaction (2), Scheme 2. TS(2) is more ionic than TS(1). The charge on the F atom that is bonded to S in **3** and to C in **2** amounts to $-0.57e$. The displacement vectors of the imaginary frequency in TS(2) show that the distance between the atoms F and S increases while the F atom approaches the C atom to which it becomes bound in **2**. The bond distance between S and F in **3** is 1.66 Å. In TS(2) this distance has increased to 2.14 Å as compared with 2.72 Å in **2**. The C–F bond distance in **2** is 1.34 Å and thus considerably smaller than the C–F distance of 2.08 Å in TS(2). The F atom that is attached to S in **3** and to C in **2** appears to be less bonded than the corresponding F atom in TS(1). The $\Delta G_{298.15}$ amounts to 275 kJ mol^{-1}. This value is considerably larger than that associated with the isomerization of **3** to **1**, and therefore it is unlikely that **3** will isomerize to **2**. Furthermore, as shown in Table 3 the activation energy identified is comparable to the energy required for the homolytic cleavage of the S–F bond. It is noted that the entropy contribution included in the $\Delta G_{298.15}$ value leads to a value for the homolytic cleavage that is 12 kJ mol^{-1} less than the activation energy in the isomerization reaction **3** to **2**.

As shown in Scheme 3 below a possible transition state has been identified for the isomerization reaction of **2** to **1**, TS(3). The value of $\Delta G_{298.15}$ for reaction (3) is 207 kJ mol^{-1}. This value is consistent with the fact that both molecules, **1** and **2**, exist as stable species. The transition state is less ionic than those of the reactions (1) and (2). The displacement vectors of the imaginary frequency in TS(3) show that the F atom approaches the C atom to which it finally becomes bound in **1**. In TS(3) the F atom

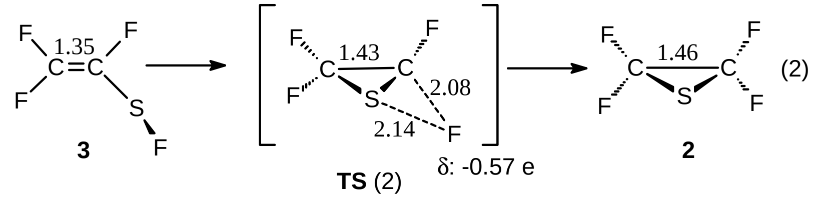

Scheme 2. The isomerization reaction **3** → **2**.

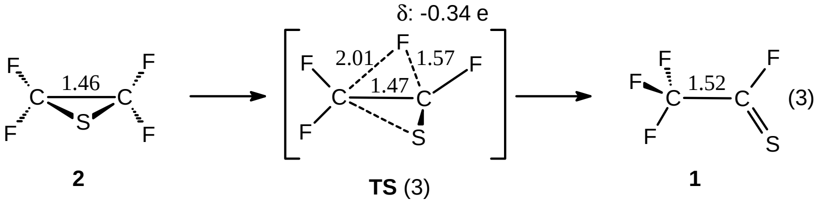

Scheme 3. The isomerization reaction **2** → **1**.

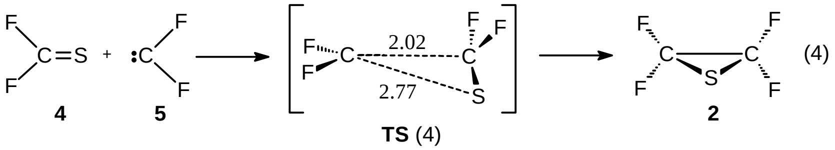

Scheme 4. Reaction between **4** and **5** to produce **2**.

that is transferred from one C to the other has acquired a charge of −0.34*e*. The bond length between C and F is 1.34 Å in **2**. This distance has increased to 1.57 Å in TS(3), but the distance to the C atom to which the F atom becomes attached is 2.01 Å. The S atom is positioned 1.65 Å from one C atom and 2.65 Å from the other C atom. Thus, in TS(3) the S atom is approaching its final position, and the reaction appears to proceed as the F atom slides along the C–C bond.

In a search for yet another transition structure, one was located that basically describes the reaction between thiocarbonyl difluoride **4** and singlet difluorocarbene **5** to produce **2**. This reaction (4) is shown in Scheme 4.

In transition structure TS(4), reaction (4), the distance between the C atoms is 2.02 Å while those between S and the two C atoms are 2.77 and 1.63 Å, respectively. The activation energy, ΔE_e, is determined as 29 kJ mol^{-1}, and $\Delta G_{298.15}$ as 81 kJ mol^{-1}. The energy gain in the reaction is derived as 172 kJ mol^{-1}. These results are consistent with the expectation that singlet difluorocarbene adds spontaneously to the C=S double bond of thiocarbonyl difluoride. However, the displacement vectors of the imaginary frequency in TS(4) show that the incipient chemical bond is between the two C atoms. This is presumably accomplished by charge flowing from the highest occupied molecular orbital of CF_2, i.e. the lone pair on C, into the lowest unoccupied orbital of $F_2C{=}S$. The non planar geometry of the transition state is essential for the constructive interactions between the frontier orbitals. Molecules and transition state structures with all the atoms of CF_2 and $S{=}CF_2$ in one plane and with either C–S–C linear or bent have also been investigated but no equilibrium geometry or transition state structure with planar geometry has been identified.

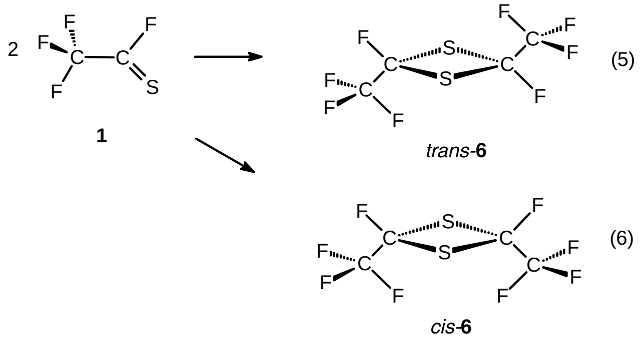

Scheme 5. The dimerization reactions, **1** → *trans*-**6** and **1** → *cis*-**6**.

Compound **1** is known to photodimerize to yield approximately equal amounts of *trans*- and *cis*-2,4-difluoro-2,4-bis(trifluoromethyl)-1,3-dithietane, *trans*-**6** and *cis*-**6**, respectively [5]. The dimerization reactions are illustrated in reactions (5) and (6) (Scheme 5).

Both dimers are thermodynamically stable relative to the monomer, and of almost equal stability. The ΔE_e and $\Delta G_{298.15}$ values determined in the G3(MP2) calculations of the dimers relative to the monomers are 115 and 45 kJ mol^{-1} for *cis*-**6**, while the corresponding values for *trans*-**6** are 112 and 44 kJ mol^{-1}. In both isomers the 1,3-dithietane ring is planar.

The results obtained in the present investigation are consistent with the fact that compounds **1** and **2** are known to be stable but suggest that **3** should also exist.

Table A.1
The total energies in au of compounds **1**–**7** as derived in HF, MP2 and G3(MP2) calculations

Compound	Symmetry	HF 6–31G*	MP2 6–31G*		G3(MP2)	Zero point energy (au)
			HF geometry (frozen core)	MP2 full optimized		
Trifluorothioacetyl fluoride, **1**	C_s	−870.97245	−872.02506	−872.06045	−872.88145	0.02375
Tetrafluorothiirane, **2**	C_{2v}	−870.93464	−871.99219	−872.02711	−872.85238	0.02351
Trifluoroethenesulfenyl fluoride, **3**(1)	C_1	−870.89989	−871.94960	−871.98536	−872.82065	0.02235
Trifluoroethenesulfenyl fluoride, **3**(2)	C_s	−870.88806	−871.93512	−871.97062	−872.80476	
Trifluoroethenesulfenyl fluoride, **3**(3)	C_s	−870.88558	−871.93325	−871.96868	−872.80354	
Thiocarbonyl fluoride, **4**	C_{2v}	−634.22382	−634.81047	−634.83429	−635.30364	0.01125
Singlet difluorocarbene, **5**	C_{2v}	−236.66074	−237.10967	−237.12047	−237.48314	0.00694
trans-2,4-Difluoro-2,4-bis(trifluoromethyl)-1,3-dithietane, *trans*-**6**	C_s	−1741.97733	−1744.09078	−1744.16130	−1745.80552	0.05059
cis-2,4-Difluoro-2,4-bis(trifluoromethyl)-1,3-dithietane, *cis*-**6**	C_{2v}	−1741.97825	−1744.09238	−1744.16305	−1745.80669	0.05063

Also included are the zero point energies.

Table A.2
The total energies in au of the transition states TS(1)–TS(4) as derived in HF, MP2 and G3(MP2) calculations

Transition state	Symmetry	HF 6–31G*	MP2 6–31G*		G3(MP2)	Zero point energy	Imaginary frequency (cm^{-1})
			HF geometry (frozen core)	MP2 full optimized			
3 → **1**, TS(1)	C_1	−870.80088	−871.88217	−871.91671	−872.74912	0.02087	773
3 → **2**, TS(2)	C_1	−870.74517	−871.83424	−871.87587	−872.71527	0.02076	479
2 → **1**, TS(3)	C_1	−870.84877	−871.90637	−871.94161	−872.77070	0.02151	464
TS(4)	C_1	−870.85954	−871.90525	−871.94270	−872.77560	0.02023	439

Also included are the zero point energies and the values of the imaginary frequencies.

Acknowledgements

The authors appreciate the computational resources provided by the Technical University of Denmark, and also by the Danish Center for Scientific Computing. The authors wish to thank one of the referees for drawing our attention to the homolytic bond cleavage in **3**.

Appendix A

See Tables A.1 and A.2.

References

[1] L.A. Curtiss, K. Raghavachari, P.C. Redfern, V. Rassolov, J.A. Pople, J. Chem. Phys. 109 (1998) 7764–7776.

[2] PC SPARTAN PRO, Wavefunction Inc., 18401 Von Karman, Suite 370, Irvine, CA 92612, USA.

[3] M.J. Frisch, G.W. Trucks, H.B. Schlegel, G.E. Scuseria, M.A. Robb, J.R. Cheeseman, V.G. Zakrzewski, J.A. Montgomery Jr., R.E. Stratmann, J.C. Burant, S. Dapprich, J.M. Millam, A.D. Daniels, K.N. Kudin, M.C. Strain, O. Farkas, J. Tomasi, V. Barone, M. Cossi, R. Cammi, B. Mennucci, C. Pomelli, C. Adamo, S. Clifford, J. Ochterski, G.A. Petersson, P.Y. Ayala, Q. Cui, K. Morokuma, N. Rega, P. Salvador, J.J. Dannenberg, D.K. Malick, A.D. Rabuck, K. Raghavachari, J.B. Foresman, J. Cioslowski, J.V. Ortiz, A.G. Baboul, B.B. Stefanov, G. Liu, A. Liashenko, P. Piskorz, I. Komaromi, R. Gomperts, R.L. Martin, D.J. Fox, T. Keith, M.A. Al-Laham, C.Y. Peng, A. Nanayakkara, M. Challacombe, P.M.W. Gill, B. Johnson, W. Chen, M.W. Wong, J.L. Andres, C. Gonzalez, M. Head-Gordon, E.S. Replogle, J.A. Pople, Gaussian Inc., Pittsburgh, PA, 2001.

[4] A. Senning, S.M. El Kousy, Sulfur Rep. 20 (1997) 197–253.

[5] W.J. Middleton, E.G. Howard, W.H. Sharkey, J. Org. Chem. 30 (1965) 1375–1384.

[6] W.R. Brasen, H.N. Cripps, C.G. Bottomley, M.W. Farlow, C.G. Krespan, J. Org. Chem. 30 (1965) 4188–4193.

[7] C.G. Krespan, W.R. Brasen, H.N. Cripps, Adv. Chem. Ser. 110 (1972) 179–189.

[8] C.G. Krespan, Chem. Sulfides Conf. 211 (1968);
C.G. Krespan, Chem. Abstr. 70 (1969) 12014.

[9] Wilkinson Sword Ltd., Neth. 19670328 (1967);
Wilkinson Sword Ltd., Chem. Abstr. 68 (1968) 14165.

[10] B. Beagley, R. Calladine, R.G. Pritchard, S.F. Taylor, J. Mol. Struct. 158 (1987) 309–314.